Title
Evaluation of a EMCCD detector for emission-transmission computed tomography

Journal
IEEE Transactions on Nuclear Science, 53(5)

ISSN
0018-9499

Authors
Teo, B K
Shestakova, I
Sun, M
et al.

Publication Date
2006-10-01

Peer reviewed

Evaluation of a EMCCD Detector for Emission-Transmission Computed Tomography

B. K. Teo, I. Shestakova, M. Sun, W. C. Barber, V. V. Nagarkar, and B. H. Hasegawa, *Member, IEEE*

***Abstract*—A prototype electron multiplying charged coupled device (EMCCD) based gamma camera is evaluated for emission-transmission computed tomography. The detector has an 8.2×8.2 mm^2 active sensor area with a 512×512 pixel array, and can be operated with a 3:1 fiber optic taper to expand the effective imaging area to approximately 25×25 mm^2 for small animal studies. We demonstrate the possibility of operating the camera in either charge integrating or single photon counting mode for pinhole SPECT with ^{125}I and ^{99m}Tc sources. In photon counting mode, we show that energy discrimination can be used to distinguish between these two sources for dual isotope imaging. X-ray CT images of phantoms are taken without a collimator to evaluate the quality of the camera for transmission imaging.**

***Index Terms*—Charge coupled device, single photon emission computed tomography, X-ray tomography.**

I. Introduction

THE ability to visualize and quantify radiopharmaceutical uptake in both humans and small animals is an important area of research in both nuclear medicine and biology. Monitoring biochemical processes through the use of radio-tracers can lead to improved diagnosis of diseases and aid in the development of new drugs. Most gamma cameras used in medical imaging today use a collimator and a scintillator coupled to an array of photomultiplier tubes. Other detectors use scintillators with silicon photodiodes, or solid-state detector materials such as cadmium zinc telluride (CZT). For these, each detector in the array requires its own electronics for processing and readout of data, which can be considerable for pixelated detectors. The spatial resolution of these cameras generally is limited to a few millimeters. For x-ray imaging, charge coupled device (CCD) image sensors have high spatial resolution, are low in cost, and have simplified image readout electronics. However, CCD detectors traditionally have been unsuitable for single-photon counting and radionuclide imaging because the readout noise incurred during the charge-to-voltage conversion process limits the sensitivity and energy-resolution of the detector.

Electron multiplying charged coupled devices (EMCCD) [1]–[3] avoid the shortcoming of conventional CCDs by incorporating an electron multiplying stage prior to the charge-to-voltage conversion process. This improves the signal to noise ratio dramatically and is particularly useful for very low light applications. The capability of single photon detection with high spatial resolution using EMCCD cameras now is having a profound impact in fields such as cellular microscopy [4] and astrophysics [5]. Because the gain can be controlled, EMCCDs also offer an extremely wide dynamic range of operation, and can be operated with either photon counting or charge integration. The simplicity of the readout electronics inherent in CCD type semiconductor sensors offer potential significant cost savings over photomultiplier tube based systems in designing a high resolution multi-detector small animal SPECT imaging system. In this study, we evaluate the the EMCCD camera (Andor iXon DV887 back illuminated) by comparing the performance, benefits, and tradeoffs of pinhole SPECT in the two acquisition modes using ^{125}I and ^{99m}Tc sources. For tests of X-ray computed tomography (CT), the electron multiplying function is turned off for regular CCD operation.

II. Detector and Collimator Requirements for SPECT/CT Imaging

A single instrument suitable for SPECT/CT [6] must satisfy the requirements of having spatial resolution better than 100 μm for CT, and good single photon sensitivity for SPECT. Our EMCCD camera is a 512×512 pixel EMCCD sensor with 16×16 μm^2 wide pixels coupled to a 3:1 fiber optic taper providing an effective imaging area of approximately 25×25 mm^2 and therefore is sufficiently large for imaging some small animals (e.g., mice). The back illuminated EMCCD chip offers increased quantum efficiency over front illuminated versions by orienting the sensitive area closer to the source to attain single photon sensitivity. While X-rays can be stopped efficiently by a thin scintillator, 500 μm thick CsI(Tl) will attenuate over 98% of 35 keV photons (^{125}I) but only about 15% of 140 keV (^{99m}Tc) photons. Thicker scintillators are required to increase the detection efficiency of 140 keV γ -rays but degrade the spatial resolution. In this study, we evaluate the EMCCD with up to 3 mm thick CsI(Tl) which can attenuate up to 70% of 140 keV γ -rays.

The collimator is a critical element in dictating both the detection efficiency and the spatial resolution of radionuclide imaging. However, the design of a small animal SPECT/CT system with a single detector is complicated since small animal SPECT typically relies on the use of a pinhole collimator which is incompatible with transmission measurements in CT. In this study, we utilize a 0.5 mm tungsten pinhole collimator for SPECT acquisition, and remove the collimator for X-ray measurements.

Manuscript received January 24, 2006; revised July 28, 2006.

B. K. Teo, M. Sun, W. C. Barber, and B. H. Hasegawa are with the Department of Radiology, Physics Research Laboratory, University of California, San Francisco, San Francisco, CA 94107 USA (e-mail: kteo@radiology.ucsf.edu; bruce.hasegawa@radiology.ucsf.edu).

I. Shestakova and V. V. Nagarkar are with Radiation Monitoring Devices, Inc., Watertown, MA 02472 USA (e-mail: vnagarkar@rmdinc.com).

Digital Object Identifier 10.1109/TNS.2006.882798

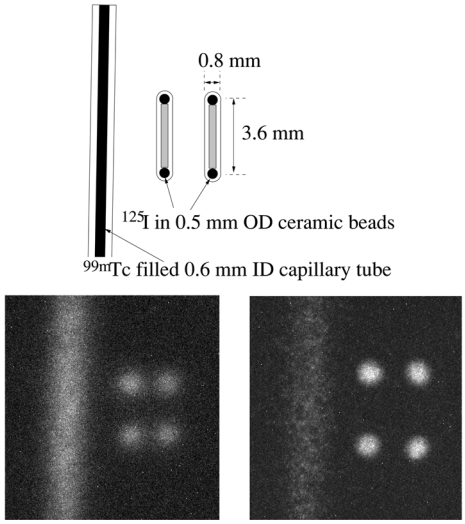

Fig. 1. Radioisotope source configuration (top) used for simultaneous imaging of 140 keV and 35 keV. The ^{99m}Tc line source and ^{125}I brachyseed images are obtained using 3 mm (bottom left) and 0.5 mm (bottom right) thick CsI(Tl) scintillators.

III. Planar Radioisotope Imaging of ^{125}I and ^{99m}Tc Sources in Integration Mode

Radionuclide images acquired using a charge integrating camera, such as a CCD, show qualitative differences from those obtained in conventional photon-counting cameras. Unlike a photon counting device, the quality of an image formed by a CCD-based gamma camera is affected by the fraction of gamma photons absorbed by the scintillator as well as the number of optical photons released per scintillation event. In the case of perfect attenuation in the scintillator, a time integrated image of two different emission sources with identical activity concentrations can appear with different intensities due to differing amounts of scintillation light collected. This can complicate quantification of the object under study with the EMCCD camera in the charge integration mode.

We first compare the relative performance of the detector using a thin scintillator for imaging low-energy photons (e.g., ^{125}I) vs. a thicker scintillator that is more suitable for imaging higher energy photons (e.g., from ^{99m}Tc). We acquired radionuclide images with the EMCCD camera coupled to a 3 mm thick CsI(Tl) microcolumnar scintillator [7] and then with the camera coupled to a 0.5 mm thick microcolumnar scintillator. These measurements were obtained by imaging (a) a 0.6 mm (inner diameter) capillary tube filled with ^{99m}Tc, and (b) two adjacent brachytherapy capsules ("Brachyseeds") as ^{125}I point sources (Fig. 1 top). The resulting radionuclide images (Fig. 1, bottom left) were obtained with the 3 mm scintillator using a 20 second exposure, and shows the ^{99m}Tc-filled line source with comparable intensities to the Brachyseeds. A similar image (Fig. 1, bottom right) recorded with a 30 second exposure using the 0.5 mm CsI (same activity levels) illustrates, as expected, the higher fraction of 35 keV relative to 140 keV photons recorded with the thin scintillator. These images have slightly different magnifications as well as object to pinhole distances and account for the slightly different spacings of the ^{125}I sources but they do not affect the qualitative differences between the planar images. A loss of spatial resolution of the line source image is also evident in the image acquired with the 3 mm scintillator, and which we attribute to parallax error (or geometrical blurring) from the non-perpendicular penetration of photons onto the scintillator as well as the lateral light spread in the thicker scintillator. While lateral light spread can be reduced with a microcolumnar scintillator [7], one can also make use of the high spatial resolution of the EMCCD to estimate the center of interaction of each scintillation event to reduce blurring from photon spread [8] in photon counting mode.

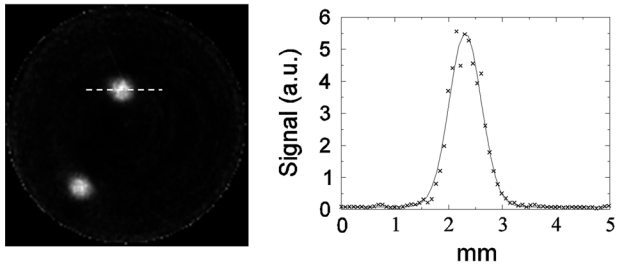

Fig. 2. Reconstructed ^{125}I brachyseed (left) and the corresponding line profile through a bead (right) shows a FWHM of 0.7 mm.

IV. SPECT of ^{125}I and ^{99m}Tc Sources in Integration Mode

Using the 0.5 mm thick scintillator, a tomographic scan of the ^{125}I Brachyseed source was acquired with 72 projections at 5 degree steps and imaged for 120 seconds per projection. The object to pinhole and pinhole to detector distances were 3.9 cm and 7.7 cm respectively. The tomograms were reconstructed using an ordered subset expectation-maximum (OSEM) algorithm (no built-in resolution recovery) with 6 iterations and 4 subsets. Fig. 2 shows a slice through one 0.5 mm bead and the corresponding profile showing a full width half maximum (FWHM) of 0.7 mm. By deconvolving the square profile of the bead from the reconstructed image, we obtain a FWHM of 0.6 mm for the point spread function of the SPECT system.

Phantom studies using two 0.6 mm diameter capillary tubes filled with ^{99m}Tc and arranged in a cross configuration at 17 degrees were imaged for 60 seconds for each of 72 projections over 360° with the 0.5 mm thick scintillator. A projection image and two slices of the reconstructed phantom using OSEM are shown in Fig. 3. The tomograms (Fig. 3 right) shows that the two capillary tubes at the intersection point (1 mm center to center) are resolved demonstrating the capability of the EMCCD camera for submillimeter SPECT resolution.

V. EMCCD Camera in Photon Counting Mode

The EMCCD camera can be operated at 35 frames per second at full resolution and more than a few hundred frames per second with on-chip binning. By operating at these high frame rates with reduced integration time, individual scintillation events can be resolved with little spatial overlap for photon counting [5], [8], [9]. A sample 0.2 second frame is shown in Fig. 4 in which multiple discrete scintillation events from ^{99m}Tc

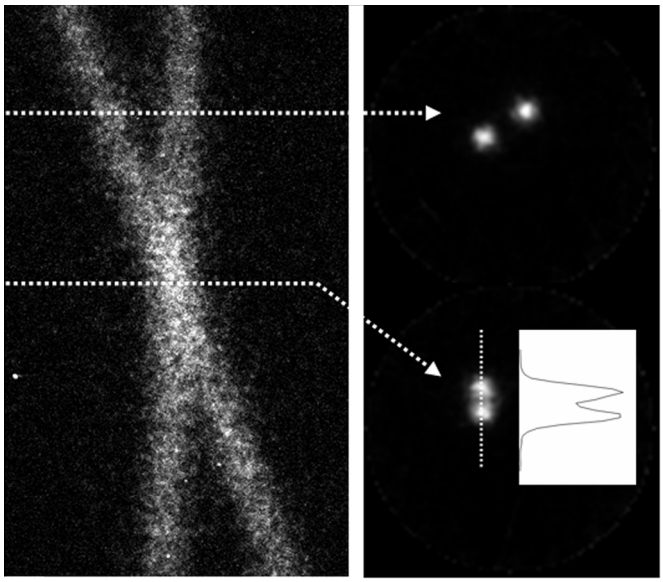

Fig. 3. Projection (left) and reconstructed (right) cross phantom filled with ^{99m}Tc.

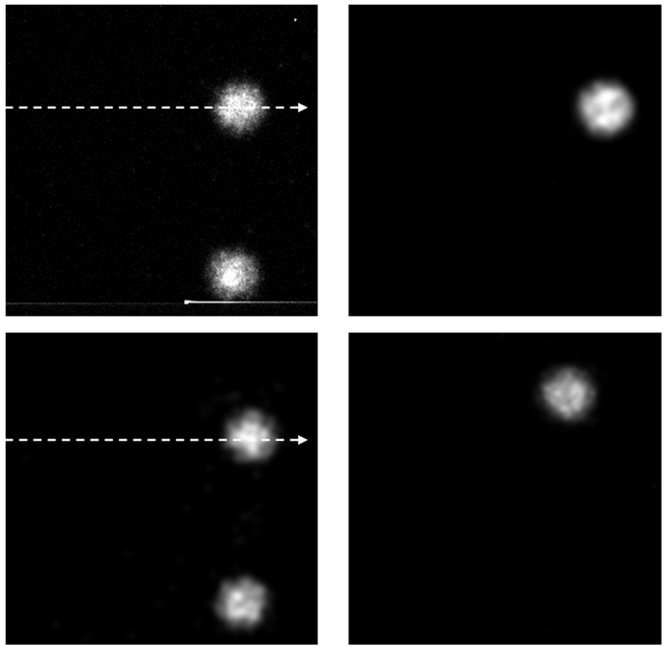

Fig. 5. Planar Images of ^{125}I sources in integration (30 seconds, top left) and photon counting (206 frames at 0.145 seconds per frame, bottom left) modes of operation. Corresponding reconstructed SPECT slices through the dotted lines are shown on the right.

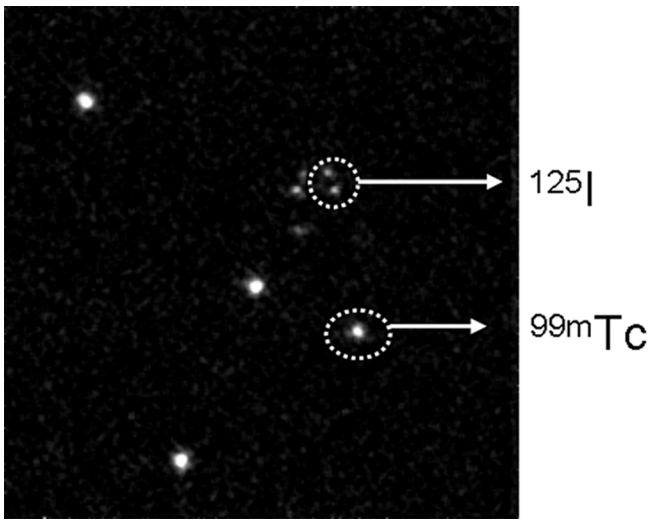

Fig. 4. Single frame with ^{125}I and ^{99m}Tc sources for photon counting of scintillation events. Each spot represents a single photon scintillation event.

and ^{125}I sources have been recorded. The relative brightness of the single events in this image is evident and indicates that this property can be used to distinguish the photon energies of the single events. Each frame is acquired in 2×2 binned mode and is processed by first subtracting a background image and then smoothing each pixel by averaging with 8 adjacent pixels. A lower threshold for the pixel value is set slightly above the noise variance and an upper threshold is set at twice the peak pixel value of scintillation events to remove hot pixels arising from direct absorption of gamma rays by the EMCCD chip. Contiguous regions with pixel values within the threshold values and whose areas are larger than 10 pixels are identified as scintillation events. The centroid, area, and peak pixel values of the events are then calculated from these post processed images. An energy distribution can be obtained from a scaled histogram matched to the known energy peaks of the source using either the summed pixel values in each event or simply by using the peak pixel value in each event.

We compared the relative performance of the EMCCD-based gamma camera in photon counting and integration modes by acquiring images of ^{125}I sources. Through photon counting, dark noise can be suppressed and direct hits eliminated. The top left image in Fig. 5 shows a projection image in integration mode with a direct hit resulting in a horizontal streak from charge spillover during the readout. This will cause artifacts in the reconstructed image if left uncorrected in the projections. In contrast, the photon counting image (Fig. 5 bottom left) shows a cleaner background with the direct hits eliminated from the photon counting algorithm. While the EMCCD can overcome the effects of readout noise, the cumulative effects of the dark noise during a long exposure can lower the image quality.

The energy resolution capability of the EMCCD camera has been described in detail in [8] for improving spatial resolution. For small animal imaging, object scatter plays a relatively minor role in affecting the SPECT image quality. We have therefore not used energy discrimination for rejecting scatter but used a broad energy window to distinguish between ^{125}I and ^{99m}Tc photons for dual isotope imaging. Using the 0.5 mm thick scintillator, we imaged two ^{99m}Tc line sources placed in front of two ^{125}I point sources. The integrated image (180 seconds) and the corresponding photon counting image (composite image from 1000 frames at 0.2 seconds per frame) are shown in Fig. 6. The ^{125}I image was separated by choosing the 10–40 keV energy window while the ^{99m}Tc image was separated using the 60–200 keV window. Due to the limited thickness of the scintillator, significantly more 35 keV photons are detected from ^{125}I than 140 keV photons from ^{99m}Tc. More importantly, Compton scatter,

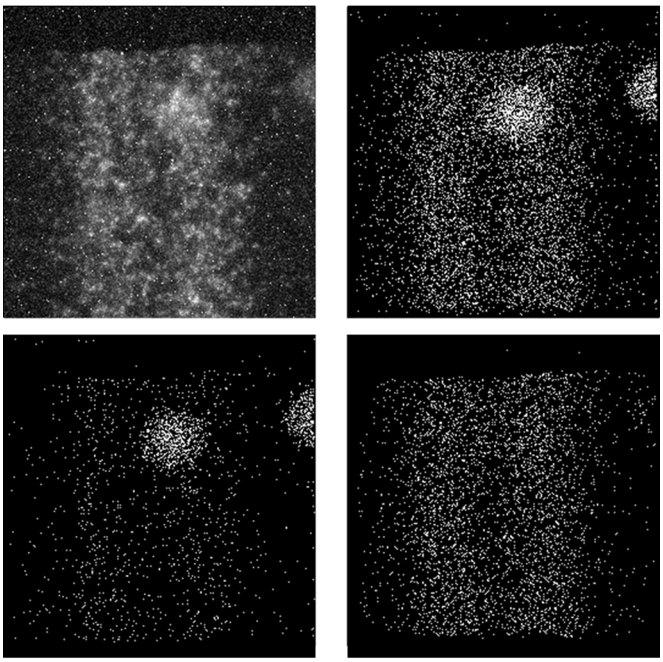

Fig. 6. Dual isotope image in integration mode (top left) and photon counting mode (top right). The bottom row shows the isotopes separated into the ^{125}I (left) and ^{99m}Tc sources (right) from the photon counting data.

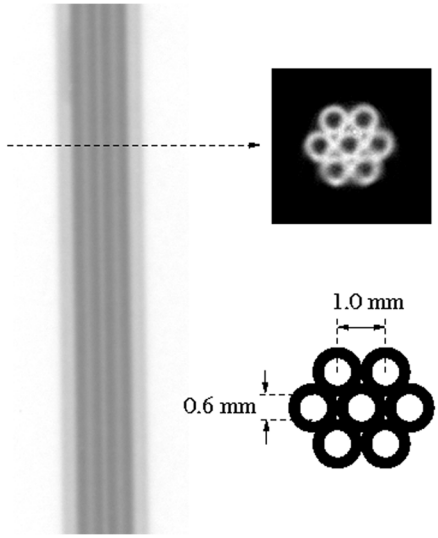

Fig. 7. X-ray CT projection (left), reconstructed image (top right) and dimensions (bottom right) of a seven barrel glass capillary tube bundle.

incomplete energy deposition of the 140 keV photons, and lower energy X-ray emissions of ^{99m}Tc can produce signals from the higher energy isotope crossing into the energy window of the lower energy isotope. We expect that a thicker scintillator will perform better in separating these two isotopes than the 0.5 mm thick scintillator. Nevertheless, these images show for the first time how an EMCCD camera has the potential for dual isotope imaging in a photon counting mode.

The electron multiplication in the gain stage of the EMCCD is a stochastic process and the excess noise factor arising from this gain stage has been shown to approach a value of 1.4 [1] for high gain settings. Due to the light spread, estimating the energy of a scintillation event by summing over all the pixel values in each event can lead to a broad distribution. We therefore have chosen to use the peak pixel value of the smoothed image to estimate the gamma energy in part because it can also tolerate some overlap between adjacent photons.

VI. EMCCD as X-Ray Camera

The electron multiplying stage of the EMCCD camera can be turned off and the low noise, high spatial resolution and dynamic range of the camera can be used for transmission imaging in X-ray CT. We qualitatively evaluated x-ray CT scans obtained with the EMCCD camera operated in current integration mode with the 0.5 mm thick scintillator. The collimator used for radionuclide imaging was removed and an X-ray tube setting of 40 kVp and 0.6 mA was used to acquire images of a phantom consisting of a bundle of seven air-filled glass capillary tubes packed in a hexagonal arrangement. In Fig. 7, a CT reconstruction using filtered backprojection of the capillary tube bundle shows excellent rendition of the hexagonal arrangement of the capillary tubes.

VII. Conclusion

We have evaluated a EMCCD-camera for CT and pinhole SPECT. This setup requires the removal of the collimator for CT measurements. A high resolution converging hole cone beam collimator focused at the X-ray source is compatible with SPECT and CT which will facilitate sequential emission-transmission measurements and produce very accurate image registration, although this approach has not been tested in this study. However, such a design involves a small tradeoff in CT sensitivity and spatial resolution. This is due to the thicker collimator septa as well as scintillator requirements for SPECT than for CT. Nevertheless, this tradeoff is minimal for a SPECT/CT system designed for imaging only low energy photons such as ^{125}I with 35 keV photons.

In conventional photon counting devices, the maximum count rate is determined by the total flux at the detector surface and thus proportional to the total injected activity in the object. For the EMCCD camera operating in photon counting mode, the maximum flux depends not on the total activity but rather on the activity concentration and image magification. In the photon counting mode, each frame certainly can handle multiple scintillation events as long as they do not overlap significantly on the detector. Thus, count rate can be increased through magnification to spatially separate multiple photons in each frame. Operating at a few hundred frames per second, activity concentrations of a few millicuries per milliliter can be imaged in photon counting mode.

The EMCCD gamma camera shows great potential for use in emission-transmission imaging. The high intrinsic resolution and relative low cost from its single readout channel makes it an attractive detector for low cost SPECT/CT systems with a single camera performing dual functions. As a gamma camera, photon

counting mode operation is possible and has advantages over integrated mode operation in terms of image quality. While good energy resolution for scatter rejection is relatively unimportant for small animal studies compared to clinical gamma cameras, having energy resolution capability can be beneficial for dual isotope *in vivo* studies of small animals.

REFERENCES

[1] M. S. Robbins and B. J. Hadwen, "The noise performance of electron multiplying charge-coupled devices," *IEEE Trans. Electron Devices*, vol. 50, no. 5, pp. 1227–1232, 2003.

[2] V. V. Nagarkar, B. Singh, I. K. Shestakova, and V. Gaysinskiy, "Design and performance of an EMCCD based detector for combined SPECT/CT imaging," in *2005 IEEE NSS/MIC Conf. Rec.*, Paper M07-254.

[3] V. V. Nagarkar, I. Shestakova, V. Gaysinskiy, S.V. Tipnis, B. Singh, W. Barber, B. Hasegawa, and G. Entine, "A CCD-based detector for SPECT'," *IEEE Trans. Nucl. Sci.*, vol. 53, no. 1, pp. 54–58, 2006.

[4] C. G. Coates, D. J. Denvir, N. G. McHale, K. D. Thornbury, and M. A. Hollywood, "Optimizing low-light microscopy with back-illuminated electron multiplying charge-coupled device: Enhanced sensitivity, speed, and resolution," *J. Biomed. Opt.*, vol. 9, no. 6, pp. 1244–1252, 2004.

[5] A. G. Basden, C. A. Haniff, and C. D. Mackay, "Photon counting strategies with low-light level CCDs," *Mon. Not. R. Astron. Soc.*, vol. 345, no. 3, pp. 985–991, 2003.

[6] T. F. Lang, B. H. Hasegawa, S. C. Liew, J. K. Brown, S. C. Blankespoor, S. M. Reilly, E. L. Gingold, and C. E. Cann, "Description of a prototype emission-transmission computed-tomography imaging system," *J. Nucl. Med.*, vol. 33, no. 10, pp. 1881–1887, 1992.

[7] V. V. Nagarkar, T. K. Gupta, S. R. Miller, Y. Klugerman, M. R. Squillante, and G. Entine, "Structured CsI(Tl) scintillators for x-ray imaging applications," *IEEE Trans. Nucl. Sci.*, vol. 45, no. 3, pp. 492–496, 1998.

[8] F. J. Beekman and G. A. de Vree, "Photon counting versus an integrating CCD-based gamma camera: Important consequences for spatial resolution," *Phys. Med. Biol.*, vol. 50, no. 12, pp. N109–N119, 2005.

[9] G. A. de Vree, A. H. Westra, I. Moody, F. van der Have, K. M. Ligtvoet, and F. J. Beekman, "Photon-counting gamma camera based on an electron-multiplying CCD," *IEEE Trans. Nucl. Sci.*, vol. 52, no. 3, pp. 580–588, 2005.